CrossMark

# Synthesis of a novel DABCO-based nanomagnetic catalyst with sulfonic acid tags: application to the synthesis of diverse spiropyrans

**Mostafa Rajabi-Salek**[1] · **Mohammad Ali Zolfigol**[1] · **Mahmoud Zarei**[1]

**Abstract** In this paper, sulfonic acid functionalized 1,4-diazabicyclo[2.2.2]octane (DABCO)-based magnetic nanoparticle $Fe_3O_4$ [$Fe_3O_4$@$SiO_2$@Pr-DABCO-$SO_3H$]$Cl_2$ was synthesized and fully characterized using various techniques. Then the catalyst was examined for the convenient synthesis of spiropyran derivatives, resulting in high reaction yields, short reaction times, and the recovery and reusability of the catalyst.

---

✉ Mohammad Ali Zolfigol
zolfi@basu.ac.ir; mzolfigol@yahoo.com

✉ Mahmoud Zarei
mahmoud8103@yahoo.com

[1] Department of Organic Chemistry, Faculty of Chemistry, Bu-Ali Sina University, Hamedan 6517838683, Iran

⊴ Springer

## Graphical Abstract
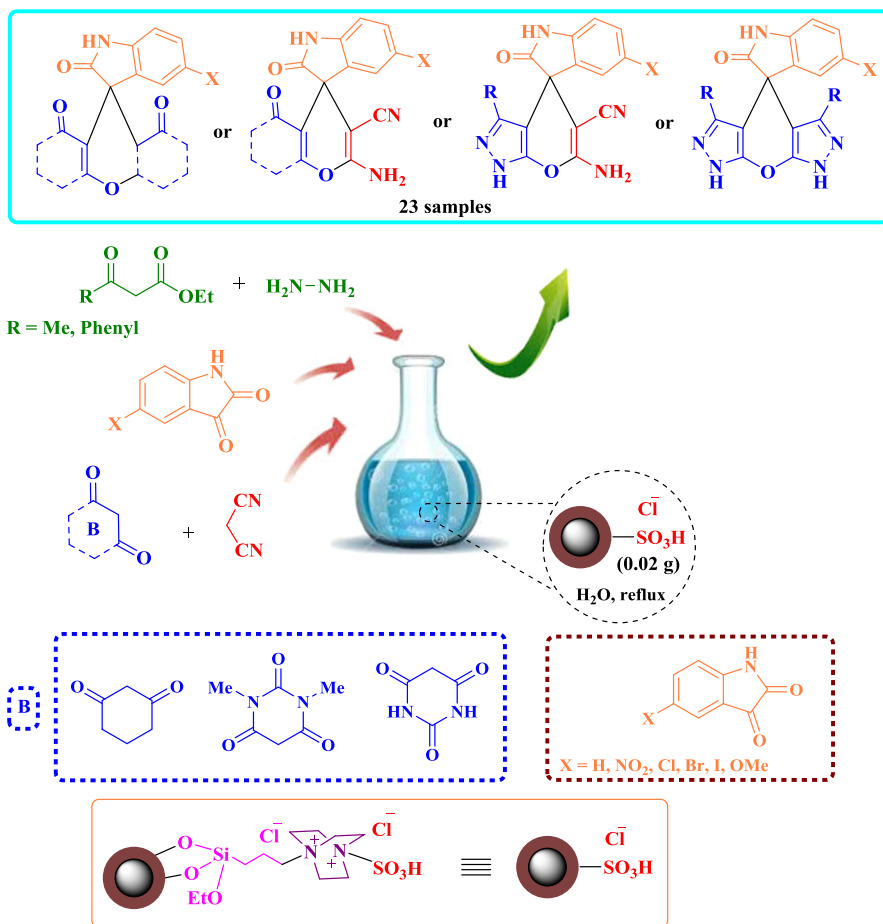


**23 samples**

## Introduction

Spiro compounds can be found in many naturally occurring substances. Likewise, the indole moiety is ubiquitous and combining the two structures can raise biological activity significantly. For example, the cytostatic alkaloids, the spirotryprostatins and pteropodines, can be noted as examples of spiroindoles [1–13]. Condensed spirooxindoles containing a condensed 4H-pyran provide pharmacologically active systems with diuretic, spasmolitic, anti-coagulant, anti-

cancer, and anti-naphylactic activities [14]. Recently, the chemistry of spirooxindoles was extensively reviewed [15]. Furthermore, nitrile substituted 4$H$-pyrans have been identified as candidates to combat neurodegenerative disorders [16, 17]. The utility of nano-magnetic catalysts is well-recognized due to the ease of work-up and catalyst recovery with such systems [18–25]. Generally, the desired catalytic active sites are immobilized on nanomagnetic $Fe_3O_4$ via coordinate or covalent bonds. $Fe_3O_4$, $Fe_3O_4$@C and $Fe_3O_4$@silica are examples of nanoparticles functionalized with $SO_3H$ groups, which have been used for various purposes [26, 27]. Recently, magnetic nanoparticles (MNPs) and mesoporous silica SBA-15 with 1,4-diazabicyclo[2.2.2]octane (DABCO) tags were also applied in organic methods [28, 29]. In a continuation of our previous work into developing of new categories of supported ionic liquids and molten salts based on nanomagnetic $Fe_3O_4$ such as silica [nano-$Fe_3O_4$@$SiO_2$@$(CH_2)_3$-Imidazole-$SO_3H$]Cl and 1,4-diazabicyclo[2.2.2]octane-sulfonic acid chloride (SBDBSAC) [30, 31], herein we decided to profit from our previous experience to design and synthesis [$Fe_3O_4$@$SiO_2$@Pr-DABCO-$SO_3H$]$Cl_2$ as an efficient nanomagnetic catalyst to be applied in the synthesis of spiropyran derivatives (Scheme 1).

# Experimental

## General information

All of the chemicals were purchased from Merck Chemical Company. The known products were identified by comparison of their melting points and spectral data with those reported in the literature. Progress of the reactions was monitored by TLC using silica gel SIL G/UV 254 plates. Melting points were recorded on a Büchi B-545 apparatus in open capillary tubes. Fourier transforms infrared (FTIR) spectra of derivatives and catalyst were recorded on a FTIR spectrometer (Perkin-Elmer spectrum 65 or JASCO FT/IR4100LE) using KBr disks. The $^1$H NMR (400 MHz)
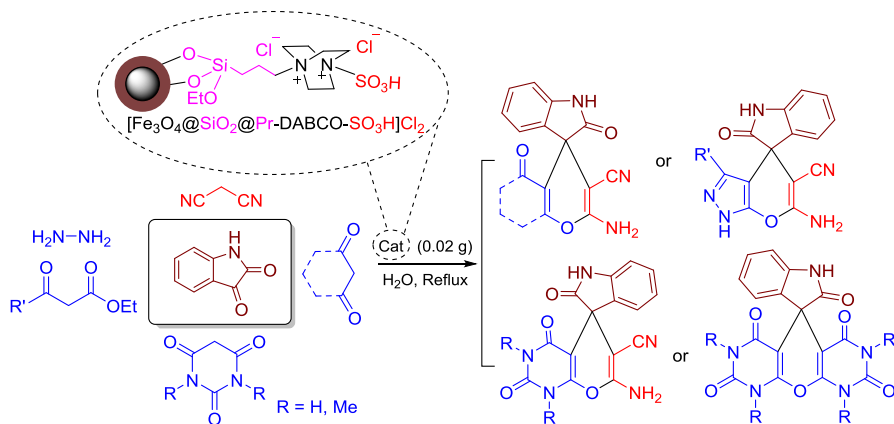


**Scheme 1** Synthesis of spiropyran derivatives using [$Fe_3O_4$@$SiO_2$@Pr-DABCO-$SO_3H$]$Cl_2$

and $^{13}C$ NMR (100 MHz) experiments were run on BRUKER BioSpin GmbH spectrometers ($\delta$ in ppm). Transmission electron microscopy (TEM) images were performed using a Zeiss-EM10C-100 microscope. Scanning electron microscopy (SEM), (EDX) and elemental mapping studies were performed using a SIGMA VP-500, VSM model LBKFB. Powder X-ray diffraction (XRD) patterns were recorded by an Ital structure ADD2000 model, using a monochromatized Cu K$\alpha$ ($\lambda = 0.154$ nm) X-ray source in the range $2° < 2\theta < 90°$. Thermogravimetric analyses were carried out on a METTLER TOLEDO apparatus (models Pyris 1) under nitrogen atmosphere at 25 °C and using a heating rate of 20 °C min$^{-1}$ up to 700 °C.

## Preparation of [Fe$_3$O$_4$@SiO$_2$@Pr-DABCO-SO$_3$H]Cl$_2$

Magnetic nanoparticles of Fe$_3$O$_4$, Fe$_3$O$_4$@SiO$_2$ and Fe$_3$O$_4$@SiO$_2$@PrCl were prepared by previously reported literature [24]. Then, 1,4-diazabicyclo[2.2.2]octane (0.491 g, 7 mmol) in dry toluene (50 mL) was added to the Fe$_3$O$_4$@SiO$_2$@PrCl (1 g) and the mixture heated to reflux for 12 h. The solid obtained was isolated using an external magnet, washed and dried accordingly to obtain [Fe$_3$O$_4$@SiO$_2$@Pr-DABCO]Cl. Finally, a solution of chlorosulfonic acid (0.456 mL, 1.165 g, 7 mmol) in dry dichloromethane (10 mL) was added drop-wise to the {Fe$_3$O$_4$@SiO$_2$@Pr-DABCO}, the reaction mixture was stirred for 6 h, isolated using an external magnet and washed with dichloromethane to give [Fe$_3$O$_4$@SiO$_2$@Pr-DABCO-SO$_3$H]Cl$_2$ (Scheme 2).

### General procedure for the synthesis of spiropyran derivatives

In a 25 mL round-bottomed flask, a mixture of isatin (1 mmol, 0.147 g), malononitrile (1 mmol, 0.066 g), 1,3-dicarbonyl compound (1 mmol), [Fe$_3$O$_4$@SiO$_2$@Pr-DABCO-SO$_3$H]Cl$_2$ (0.02 g) and H$_2$O (10 mL) were added a fitted reflux condenser. The mixture was heated to reflux and, after completion of the reaction (monitoring by TLC), the mixture was allowed to cool to room temperature, and the solvent was removed under vacuum. Then, the resultant solid mixture was extracted with acetone (10 mL), and the catalyst was recovered using an external magnet. The obtained pure products were washed with water/ethanol (Scheme 1).

## Result and discussion

At the outset, we chose to synthesise heterogeneous nanomagnetic [Fe$_3$O$_4$@SiO$_2$@Pr-DABCO-SO$_3$H]Cl$_2$. Magnetic nanoparticles of Fe$_3$O$_4$, Fe$_3$O$_4$@SiO$_2$ and Fe$_3$O$_4$@SiO$_2$@PrCl were synthesized according to the previously reported procedure [24]. Then, 1,4-diazabicyclo[2.2.2]octane was added to the Fe$_3$O$_4$@SiO$_2$@PrCl and nanomagnetic [Fe$_3$O$_4$@SiO$_2$@Pr-DABCO]Cl was isolated. In the next step, a solution of chlorosulfonic acid in dry dichloromethane was added drop-wise to the suspension of {Fe$_3$O$_4$@SiO$_2$@Pr-DABCO}, the reaction mixture filtered, and the precipitate was washed with dichloromethane to give the desired
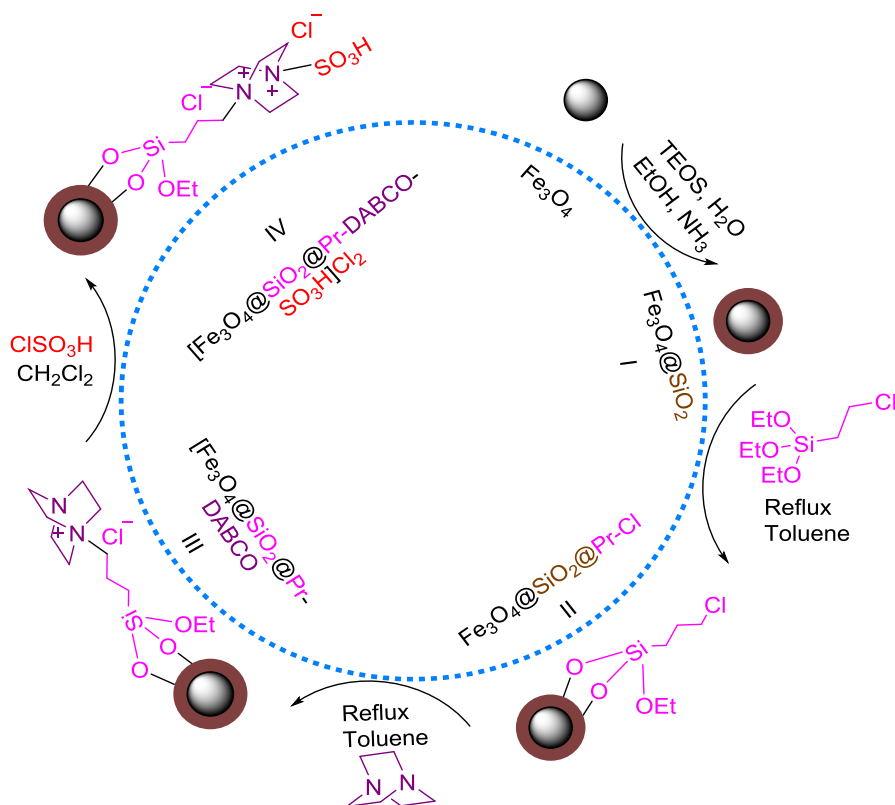
**Scheme 2** Schematic preparation route of [Fe$_3$O$_4$@SiO$_2$@Pr-DABCO-SO$_3$H]Cl$_2$

[Fe$_3$O$_4$@SiO$_2$@Pr-DABCO-SO$_3$H]Cl$_2$. This material was characterized using FT-IR, X-ray diffraction patterns (XRD), SEM with elemental mapping and EDX, TEM, TG/DTG and VSM.

In the FT-IR spectrum of [Fe$_3$O$_4$@SiO$_2$@Pr-DABCO-SO$_3$H]Cl$_2$, a broad band at 2600–3500 cm$^{-1}$ was assigned to the OH stretching frequency of the SO$_3$H group [32, 33]. The observation of a broad band at 1094–1222 cm$^{-1}$ indicated the presence of SiO$_2$ bands and two peaks at 1087 and 1206 cm$^{-1}$ corresponded to the vibrational modes of N–SO$_2$ and O–SO$_2$ bonds overlapped with SiO$_2$ bands (Fig. 1).

The particle size and shape as well as the morphology of [Fe$_3$O$_4$@SiO$_2$@Pr-DABCO-SO$_3$H]Cl$_2$ as examined by XRD, SEM, SEM-elemental mapping, EDX and TEM are shown in Figs. 2, 3, 4, 5, and 6 and Table 1. The X-ray diffraction profile of [Fe$_3$O$_4$@SiO$_2$@Pr-DABCO-SO$_3$H]Cl$_2$ was screened in a domain of 2° to 90°. The crystallite size was calculated using the Debye–Sherrer formula $D = K\lambda/(\beta Cos\theta)$ [34] and was found to be in the range 14–81 nm (Table 1 and Fig. 2), which is in a close agreement with the scanning electron microscopy results (SEM) (Fig. 3).

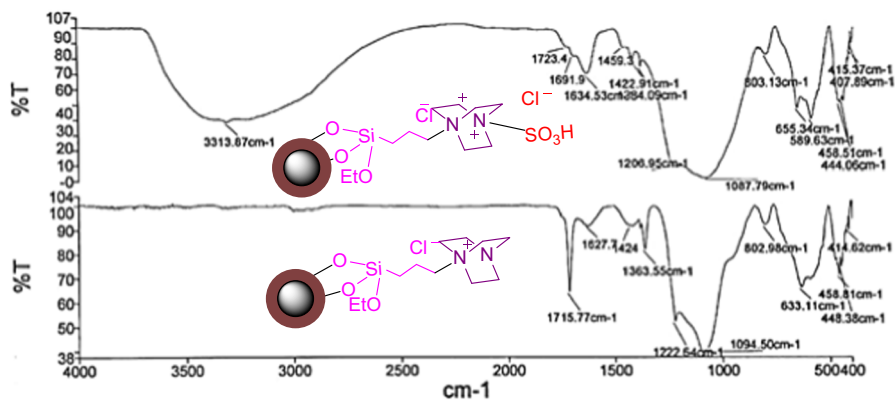**Fig. 1** FT-IR spectra of [Fe$_3$O$_4$@SiO$_2$@Pr-DABCO-SO$_3$H]Cl$_2$ compared with steps of intermediate III
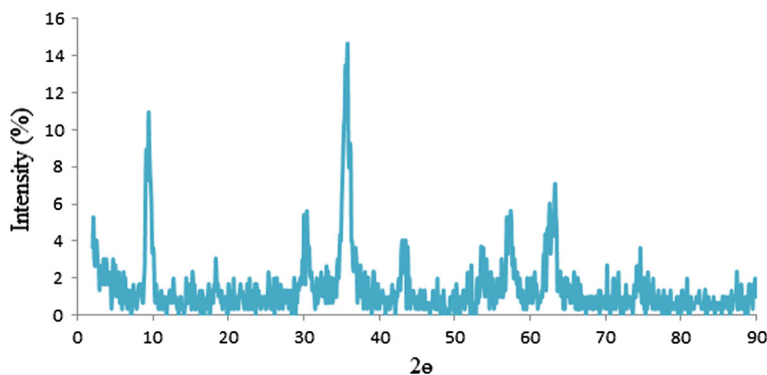


**Fig. 2** XRD pattern of [Fe$_3$O$_4$@SiO$_2$@Pr-DABCO-SO$_3$H]Cl$_2$

**Table 1** XRD data for [Fe$_3$O$_4$@SiO$_2$@Pr-DABCO-SO$_3$H]Cl$_2$

| Entry | $2\theta$ | Peak width (°) | Size (nm) | Inter planar distance (nm) |
|---|---|---|---|---|
| 1 | 9.1 | 0.4 | 13.8 | 0.98 |
| 2 | 18.3 | 0.1 | 24.3 | 0.12 |
| 3 | 30.1 | 0.2 | 28.7 | 0.19 |
| 4 | 35.8 | 0.7 | 81.1 | 0. 98 |
| 5 | 43.0 | 0.2 | 32.1 | 0.12 |
| 6 | 57.2 | 0.3 | 30.1 | 0.16 |
| 7 | 63.3 | 0.4 | 23.7 | 0.14 |

Using SEM elemental mapping and EDX, the presence of C, N, O, Fe, S, Si and Cl with a good distribution over the catalyst surface was also verified (Figs. 4 and 5). TEM analysis (Fig. 6) indicated well-dispersed nanospherical particles with an average size of 60 nm. Magnetic measurements showed that saturation of the catalyst dropped to 27.6 emu g$^{-1}$ for [Fe$_3$O$_4$@SiO$_2$@Pr-DABCO-SO$_3$H]Cl$_2$ compared to Fe$_3$O$_4$ at 68.8 emu g$^{-1}$ (Fig. 7).
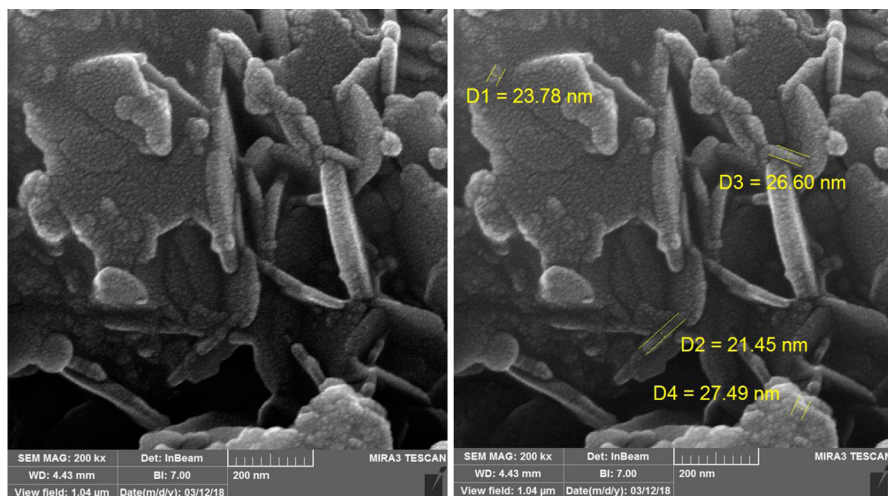
**Fig. 3** SEM of [$Fe_3O_4$@$SiO_2$@Pr-DABCO-$SO_3H$]$Cl_2$

Thermal gravimetric analysis and differential thermal gravimetric profiles are presented in Fig. 8. In the TGA, the first weight loss step, relating to the loss of surface-adsorbed water and organic solvents, takes place between 25 and 105 °C and involves a weight loss of 3%. Finally, the second and main weight loss between 105 and 500 °C can be ascribed to the continuous decomposition of the organic components (Fig. 8).

After approving the structure of described catalyst, we decided to study its catalytic activity in the synthesis of spiropyran derivatives. For initial screening of the catalytic applications, a multicomponent reaction between 1 mmol of isatin, malononitrile and barbituric acid was considered as a model reaction (Table 2). Low yield was obtained in the absence of catalyst under refluxing water conditions (Table 2, entry 1). The optimal catalyst loading was (0.02 g) (Table 2, entry 5). For solvent optimization, the model reaction was carried out using $H_2O$, $CHCl_3$, EtOH, EtOAc, Toluene and $CH_3CN$ under reflux conditions. As summarized in Table 2 (entries 11–16), applying the refluxing water conditions afforded better yields and reaction times than other reactions media.
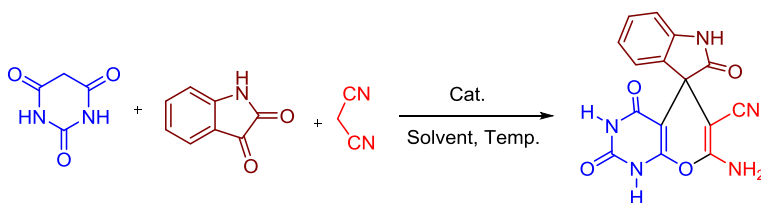


Aiming to extend the scope and generality of the described protocol, after optimization of the reaction conditions, a series of isatins was reacted with

EDS Layered Image 4
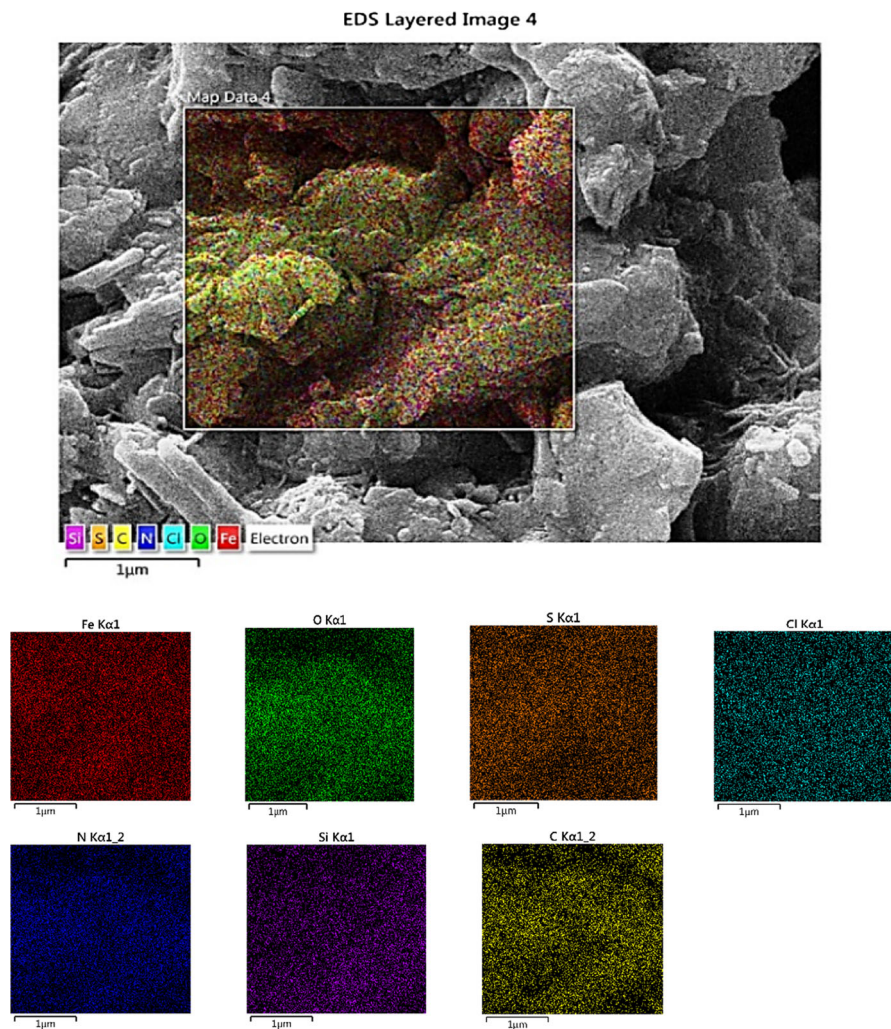


**Fig. 4** SEM-elemental mapping of Fe, O, S, Cl, N Si and C atoms for [Fe$_3$O$_4$@SiO$_2$@Pr-DABCO-SO$_3$H]Cl$_2$

malononitrile, 1,3-dicarbonyl compounds, hydrazine, ethyl benzoylacetate and ethyl acetoacetate under the optimized conditions. The results are presented in Table 3. All reactions proceeded efficiently to give the desired spiropyran derivatives in good to excellent yields and in short reaction times.
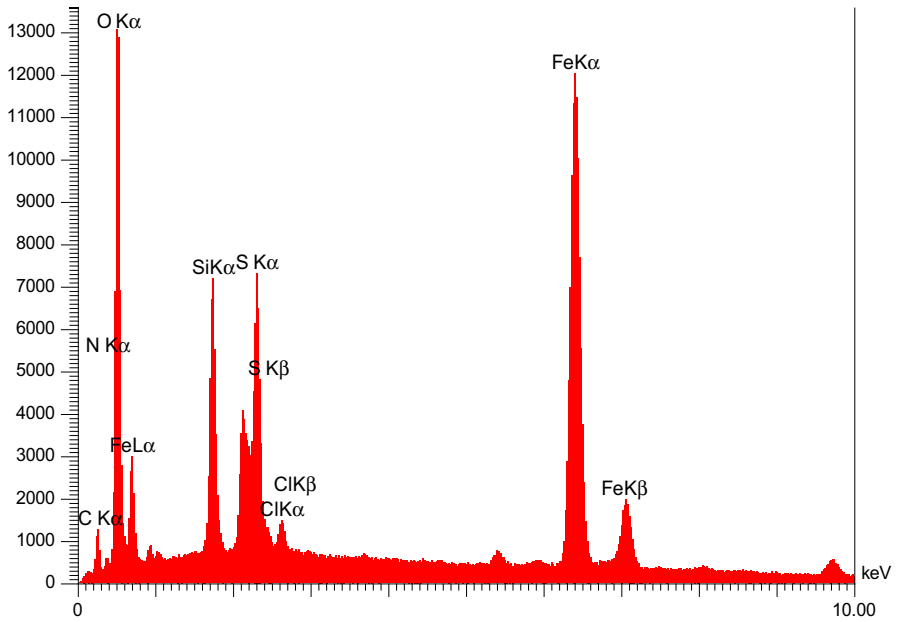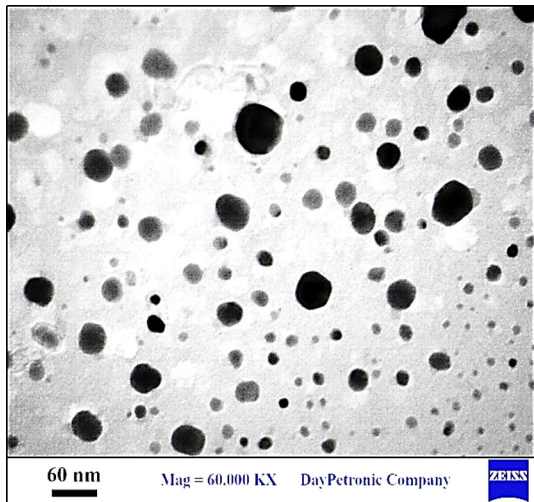
**Fig. 5** EDX of $[Fe_3O_4@SiO_2@Pr\text{-}DABCO\text{-}SO_3H]Cl_2$

**Fig. 6** TEM of $[Fe_3O_4@SiO_2@Pr\text{-}DABCO\text{-}SO_3H]Cl_2$
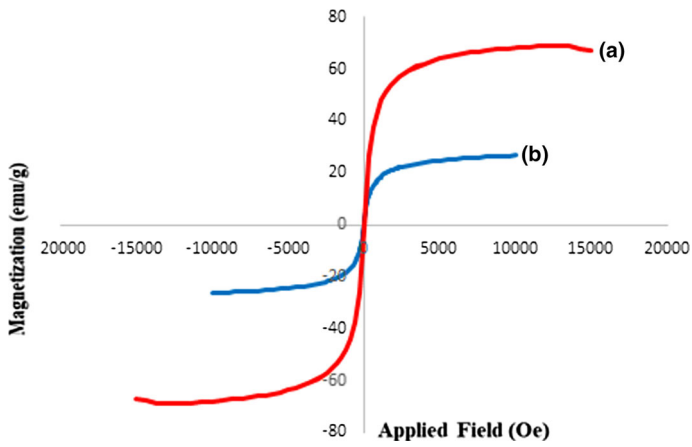
Fig. 7 VSM of a $Fe_3O_4$ (red) and b $[Fe_3O_4@SiO_2@Pr\text{-}DABCO\text{-}SO_3H]Cl_2$ (blue). (Color figure online)
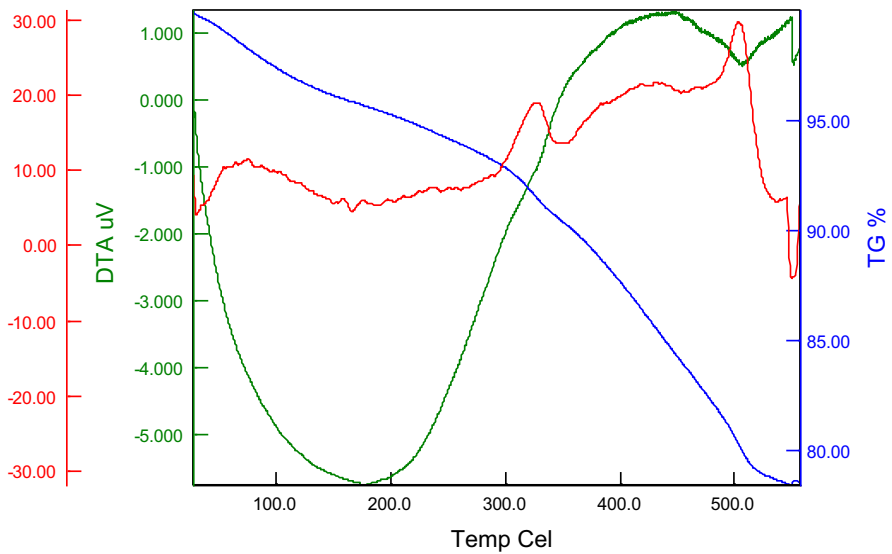


Fig. 8 Differential thermal analysis (TG/DTA) of $[Fe_3O_4@SiO_2@Pr\text{-}DABCO\text{-}SO_3H]Cl_2$

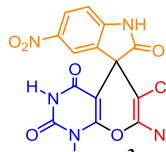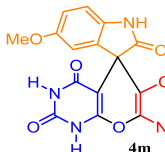**Table 2** The optimization of catalyst loading, temperature and various solvents (10 ml) in the synthesis of spiropyrans
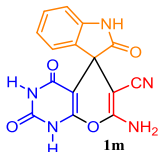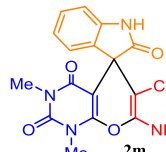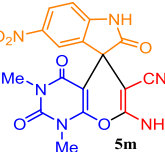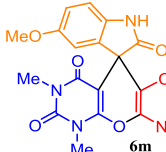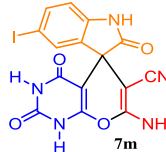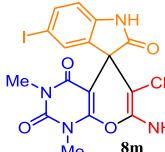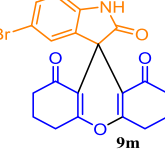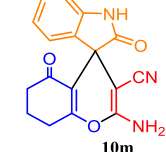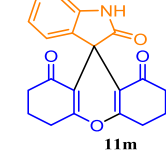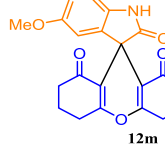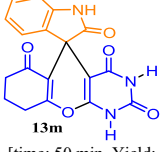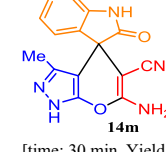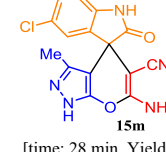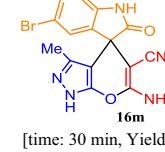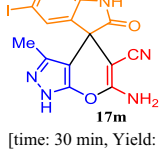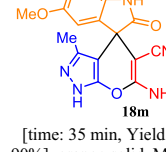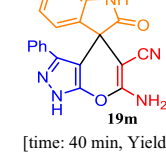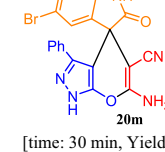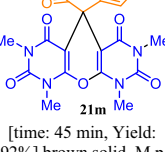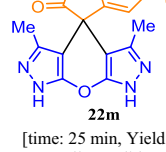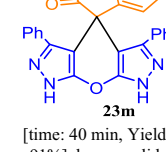
| Entry | Amount of catalyst (g) | Solvent | Temp. (°C) | Time (min) | Yield[a] (%) |
|---|---|---|---|---|---|
| 1 | – | $H_2O$ | Reflux | 400 | 33 |
| 2 | 0.005 | $H_2O$ | Reflux | 110 | 62 |
| 3 | 0.01 | $H_2O$ | Reflux | 80 | 75 |
| 4 | 0.015 | $H_2O$ | Reflux | 50 | 80 |
| 5 | 0.02 | $H_2O$ | Reflux | 30 | 95 |
| 6 | 0.025 | $H_2O$ | Reflux | 35 | 95 |
| 7 | 0.03 | $H_2O$ | Reflux | 35 | 95 |
| 8 | 0.02 | $H_2O$ | rt | 140 | 65 |
| 9 | 0.02 | $H_2O$ | 40 | 40 | 87 |
| 10 | 0.02 | $H_2O$ | 70 | 38 | 91 |
| 11 | 0.02 | EtOH | Reflux | 40 | 90 |
| 12 | 0.02 | $CHCl_3$ | Reflux | 100 | 80 |
| 13 | 0.02 | EtOAc | Reflux | 60 | 60 |
| 14 | 0.02 | Toluene | Reflux | 70 | 20 |
| 15 | 0.02 | $CH_3CN$ | Reflux | 60 | 10 |
| 16 | 0.02 | – | 100 | 60 | N.R |
| 16 | 0.02 | – | 100 | 60 | N.R |

[a]Isolated yield

A plausible mechanism for the reaction is indicated in Scheme 3. Initially, the carbonyl group of isatin is activated by the acidic moiety of [$Fe_3O_4$@$SiO_2$@Pr-DABCO-$SO_3H$]$Cl_2$ (i.e., $SO_3H$), suffers a Knoevenagel condensation with the activated malononitrile compound, which was followed by removing one molecule of $H_2O$ to give intermediate I. 1,3-Dicarbonyl compounds (B) is converted to enol form after tautomerisation and attached to cyanoolefin compound (**I**), as a Michael acceptor, to give **II**. Finally, there was a cyclocondensation reaction of **II** prepared **III**, which is converted to the corresponding product via tautomerization.

The recyclability and reuse of the catalyst was also studied in the model reaction. As indicated in Fig. 9, [$Fe_3O_4$@$SiO_2$@Pr-DABCO-$SO_3H$]$Cl_2$ was successfully recycled and efficiently reused for up to eight reaction cycles with only a moderate decrease in its catalytic activity. The acidic content of [$Fe_3O_4$@$SiO_2$@Pr-DABCO-$SO_3H$]$Cl_2$ was determined by titration against aqueous NaOH [42].

**Table 3** The preparation of spiropyran derivatives using [Fe₃O₄@SiO₂@Pr-DABCO-SO₃H]Cl₂ as a novel nano magnetic catalyst in water and under reflux conditions



**1m**
[time: 30 min, Yield: 95%], white solid, M.p (˚C): 268-270 [35]

**2m**
[time: 30 min, Yield: 95%], brown solid, M.p (˚C): 232-234 [35]

**3m**
[time: 30 min, Yield: 91%], yellow solid, M.p (˚C): 276-278 [36]

**4m**
[time: 35 min, Yield: 95%], yellow solid, M.p (˚C): 212-214 [39]

**5m**
[time: 37 min, Yield: 96%] yellow solid, M.p (˚C): 264-266[36]

**6m**
[time: 30 min, Yield: 95%] brown solid, M.p (˚C): 268-270

**7m**
[time: 36 min, Yield: 98%] brown solid, M.p (˚C): 252-254[36]

**8m**
[time: 37 min, Yield: 93%], yellow solid, M.p (˚C): 239-242[36]

**9m**
[time: 45 min, Yield: 94%], brown solid, M.p (˚C): >300

**10m**
[time: 55 min, Yield: 91%], white solid, M.p (˚C): 278-280 [9]

**11m**
[time: 44 min, Yield: 88%], orange solid, M.p (˚C): >300 [40]

**12m**
[time: 45 min, Yield: 95%], brown solid, M.p (˚C): >300

**13m**
[time: 50 min, Yield: 93%], orange solid, M.p (˚C): >300 [11]

**14m**
[time: 30 min, Yield: 96%], yellow solid, M.p (˚C): 286-288 [37]

**15m**
[time: 28 min, Yield: 94%], yellow solid, M.p (˚C): 318-320 [38]

**16m**
[time: 30 min, Yield: 95%], orange solid, M.p (˚C): 326-328 [38]

**17m**
[time: 30 min, Yield: 94%], brown solid, M.p (˚C): 318-320 [41]

**18m**
[time: 35 min, Yield: 90%], orange solid, M.p (˚C): 260-262 [41]

**19m**
[time: 40 min, Yield: 91%], brown solid, M.p (˚C): 276-278 [38]

**20m**
[time: 30 min, Yield: 97%], orange solid, M.p (˚C): 283-285 [11]

**21m**
[time: 45 min, Yield: 92%] brown solid, M.p (˚C): >300

**22m**
[time: 25 min, Yield: 96%] yellow solid, M.p (˚C): 273-275

**23m**
[time: 40 min, Yield: 91%], brown solid, M.p (˚C): 214-216
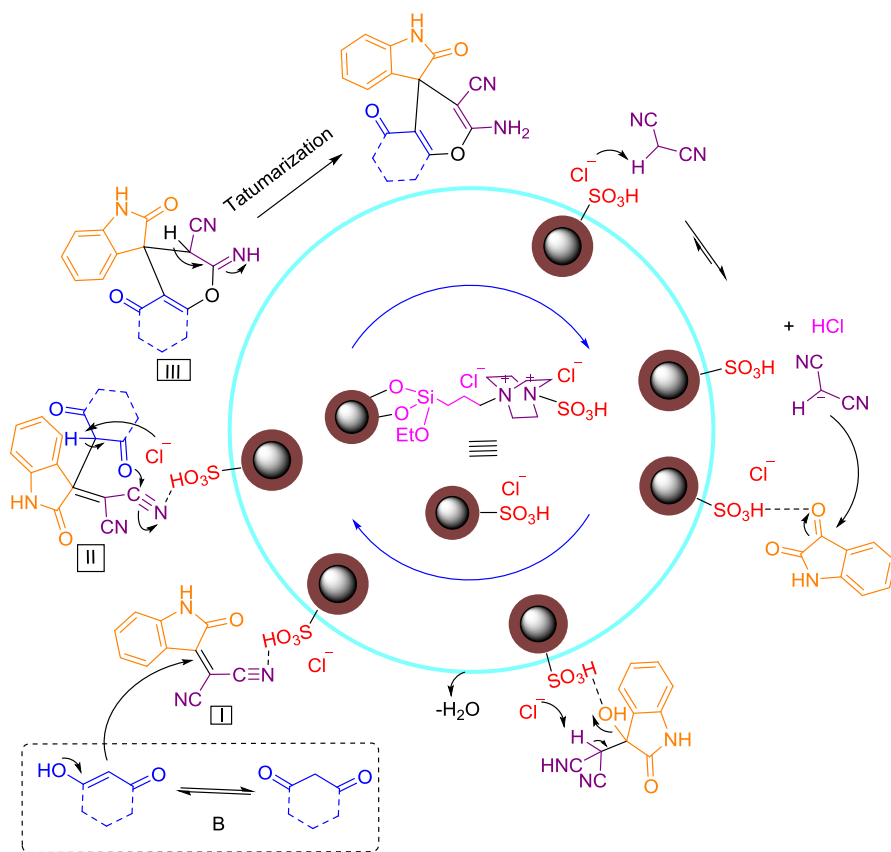
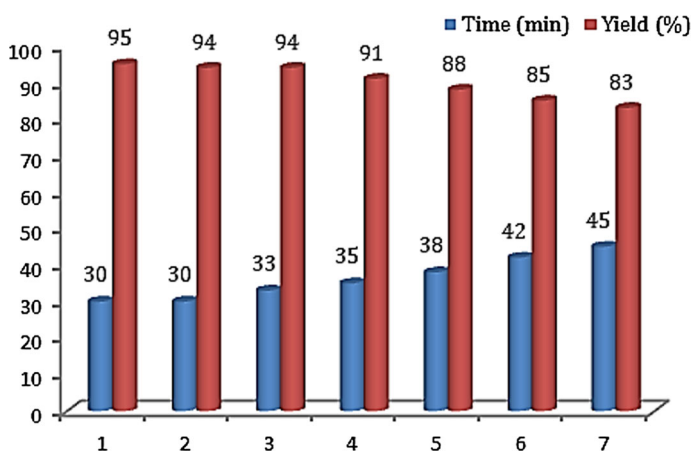**Scheme 3** The proposed mechanism for the synthesis of spiropyrans



**Fig. 9** Recyclability of [Fe₃O₄@SiO₂@Pr-DABCO-SO₃H]Cl₂

## Conclusion

In conclusion, a convenient procedure is presented for the synthesis of spiropyran derivatives in the presence of $[Fe_3O_4@SiO_2@Pr-DABCO-SO_3H]Cl_2$ as a novel nanomagnetic catalyst in refluxing water. The catalyst was fully characterized by FT-IR, XRD, TEM, SEM-elemental mapping, EDX, TG/DTG and VSM. High yield of products, short reaction time, facile workup and reusability of the catalyst are major advantages of the described work.

## References

1. M. Shiri, Chem. Rev. **3508**, 112 (2012)
2. W. Francke, W. Kitching, Curr. Org. Chem. **233**, 5 (2001)
3. S. Rosenberg, R. Leino, Synthesis **2651**, 262 (2009)
4. R.M. Williams, R.J. Cox, Acc. Chem. Res. **127**, 36 (2003)
5. D. Silva, J.F.M. Garden, S.J. Pinto, J. Braz. Chem. Soc. **12**, 273 (2001)
6. C. Marti, E.M. Carreira, Eur. J. Org. Chem. **2209**, 63 (2003)
7. A.B. Dounay, K. Hatanaka, J.J. Kodanko, M. Oestreich, L.E. Overman, L.A. Pfeifer, M.M. Weis, J. Am. Chem. Soc. **6261**, 125 (2003)
8. A. Khalafi-Nezhad, E. Shaikhi Shahidzadeh, S. Sarikhani, F. Panahi, J. Mol. Catal. A. Chem. **379**, 1 (2013)
9. G. Rui-Yun, A. Zhi-Min, W. Li-Ping, W. Rui-Zhi, L. Hong-Xia, W. Shu-Xia, Z. Zhan-Hui, ACS Comb. Sci. **557**, 15 (2013)
10. S. Ahadi, Z. Yasaei, A. Bazgir, J. Heterocyclic Chem. **1090**, 47 (2010)
11. A.R. Moosavi-Zare, M.A. Zolfigol, E. Noroozizadeh, M. Zarei, R. Karamian, M. Asadbegy, J. Mol. Catal. A: Chem. **217**, 425 (2016)
12. D.S. Raghuvanshi, K.N. Singh, J. Heterocyclic Chem. **1323**, 47 (2010)
13. P.S. Satasia, P.N. Kalaria, J.R. Avalani, D.K. Raval, Tetrahedron **5763**, 70 (2014)
14. W.P. Smith, L.S. Sollis, D.P. Howes, C.P. Cherry, D.I. Starkey, N.K. Cobley, J. Med. Chem. **787**, 41 (1998)
15. L.J. Yan, Y.C. Wang, Chemistry Select. **6948**, 1 (2016)
16. L. Bonsignore, G. Loy, D. Secci, A. Calignano, Eur. J. Med. Chem. **515**, 28 (1993)
17. L. Andreani, E. Lapi, Bol. Chim. Farm. **583**, 99 (1960)
18. T. Cheng, D. Zhang, H. Li, G. Liu, Green Chem. **3401**, 16 (2014)
19. R. Mrowczynski, A. Nan, J. Liebscher, RSC Adv. **5927**, 4 (2014)
20. M.A. Zolfigol, V. Khakyzadeh, A.R. Moosavi-Zare, A. Rostami, A. Zare, N. Iranpoor, M.H. Beyzavi, R. Luque, Green Chem. **2132**, 15 (2013)
21. D. Zhang, C. Zhou, Z. Sun, L.-Z. Wu, C.-H. Tung, T. Zhang, Nanoscale **6244**, 4 (2012)
22. V. Polshettiwar, R. Luque, A. Fihri, H. Zhu, M. Bouhrara, J.-M. Basset, Chem. Rev. **3036**, 111 (2011)
23. K. Debnath, K. Singha, A. Pramanik, RSC Adv. **31866**, 5 (2015)
24. S. Moradi, M.A. Zolfigol, M. Zarei, D.A. Alonso, A. Khoshnood, A. Tajally, Appl. Organomet. Chem. **32**, e4084 (2018)
25. M. Mokhtary, J. Iran. Chem. Soc. **1827**, 13 (2016)
26. A. Khorshidi, S. Shariati, M. Aboutalebi, N. Mardazad, Iran. Chem. Commun. **476**, 4 (2016)
27. C. Zhang, H. Wang, F.L. Liu, H.He Wang, Cellulose **127**, 20 (2013)
28. A. Ying, S. Liu, Y. Ni, F. Qiu, S. Xu, W. Tang, *Catal. Sci. Technol.* **2115**, 4 (2014)
29. R. Baharfar, R. Azimi, Synth. Commun. **44**, 89 (2014)
30. M.A. Zolfigol, R. Ayazi-Nasrabadi, S. Baghery, V. Khakyzadeh, S. Azizian, J. Mol. Catal. A: Chem. **54**, 418 (2016)

31. A.R. Moosavi-Zare, M.A. Zolfigol, E. Noroozizadeh, R. salehi Moratab, M. Zarei. J. Mol. Catal. A: Chem. **246**, 420 (2016)
32. A.R. Moosavi-Zarea, M.A. Zolfigol, M. Zarei, A. Zare, V. Khakyzadeh, A. Hasaninejad, Applied Catal A: Gen. **467**, 61 (2013)
33. A.R. Moosavi-Zarea, M.A. Zolfigol, M. Zarei, A. Zare, J. Afsar, Applied Catal A: Gen. **505**, 224 (2015)
34. M.A. Zolfigol, S. Baghery, A.R. Moosavi-Zare, S.M. Vahdat, J. Mol. Catal. A: Chem. **216**, 409 (2015)
35. R.-Y. Guo, Z.-M. An, L.-P. Mo, R.-Z. Wang, H.-X. Liu, S.-X. Wang, Z.H. Zhang, ACS Comb. Sci. **557**, 15 (2013)
36. R.D. Chandam, G.M. Abhijeet, R.P. Dayanand, B.D. Madhukar, Res. Chem. Intermed. **1411**, 42 (2015)
37. J. Feng, K. Ablajan, A. Sali, Tetrahedron **484**, 70 (2014)
38. S.F. Hojati, H. Raouf, Org. Prep. Proc. Int. **474**, 48 (2016)
39. N.G. Singh, M. Lily, S.P. Devi, N. Rahman, A. Ahmed, A.K. Chandra, R. Nongkhlaw, Green Chem. **4216**, 18 (2016)
40. K.C. Joshi, R. Jain, S. Aroma, J. Fluorine Chem. **149**, 42 (1989)
41. D.M. Pore, P.G. Hegade, D.S. Gaikwad, P.B. Patil, J.D. Patil, Lett. Org. Chem. **131**, 11 (2014)
42. A.R. Moosavi-Zare, M.A. Zolfigol, M. Zarei, A. Zare, J. Afsar, Appl. Catal. A **224**, 505 (2015)